Late-Time Mixing Sensitivity to Initial Broadband Surface Roughness in High-Energy-Density Shear Layers

K. A. Flippo,[1,*] F. W. Doss,[2,†] J. L. Kline,[1] E. C. Merritt,[1] D. Capelli,[3] T. Cardenas,[3] B. DeVolder,[4] F. Fierro,[3] C. M. Huntington,[5] L. Kot,[1] E. N. Loomis,[1] S. A. MacLaren,[5] T. J. Murphy,[1] S. R. Nagel,[5] T. S. Perry,[1] R. B. Randolph,[3] G. Rivera,[3] and D. W. Schmidt[3]

[1]*Physics Division, Plasma Physics, Los Alamos National Laboratory, Los Alamos, New Mexico 87545, USA*
[2]*Theoretical Design Division, Los Alamos National Laboratory, Los Alamos, New Mexico 87545, USA*
[3]*Materials Science and Technology Division, Los Alamos National Laboratory, Los Alamos, New Mexico 87545, USA*
[4]*Computational Physics Division, Los Alamos National Laboratory, Los Alamos, New Mexico 87545, USA*
[5]*Lawrence Livermore National Laboratory, Livermore, California 94550-9234, USA*

(Received 22 March 2016; published 23 November 2016)

Using a large volume high-energy-density fluid shear experiment (8.5 cm^3) at the National Ignition Facility, we have demonstrated for the first time the ability to significantly alter the evolution of a supersonic sheared mixing layer by controlling the initial conditions of that layer. By altering the initial surface roughness of the tracer foil, we demonstrate the ability to transition the shear mixing layer from a highly ordered system of coherent structures to a randomly ordered system with a faster growing mix layer, indicative of strong mixing in the layer at a temperature of several tens of electron volts and at near solid density. Simulations using a turbulent-mix model show good agreement with the experimental results and poor agreement without turbulent mix.

DOI: 10.1103/PhysRevLett.117.225001

Introduction.—In compressible high-energy-density (HED) flows it has been generally assumed, as with early fluid turbulence analysis, that the self-similar conditions would quickly wipe out the initial conditions of the flow with the onset of turbulence [1] and all solutions would collapse into one universal solution based only on local flow properties. This has been especially true for HED experiments, where it was thought that the energetic particle or photon preheat would tend to wash out any small scale initial conditions, therein moving the layer quickly to a more or less universal system. Here, in an HED experiment, it is shown not to be the case: rather, the initial conditions keep the system from evolving into a universal state or even becoming self-similar on longer than anticipated time scales, similar to what was previously shown in fluid turbulence [2]. We report on experiments carried out at the National Ignition Facility (NIF) laser system [3], which is capable of delivering over 1.8 MJ of laser light on a target, following the evolution of a mixing layer [4–7] created inside a large volume HED shock tube at tens of electron volts in temperature with a counterflowing shear geometry. These are the first HED experiments to observe coherent structures evolving from the inherent roughness in the system and demonstrate that, by controlling the initial surface structure, the mix can be forced from a highly coherent state to a strongly isotropic state indicative of developed turbulence. In this experiment, we use ∼600 kJ of laser energy converted into a 250 eV thermal bath of soft x rays to drive both sides of a shock tube (see Fig. 1) with counterpropagating 10 Mbar shocks establishing a counterstreaming shear flow of 100 km/s on both sides of a mixing tracer layer. This experiment is unique for an HED hydroexperiment in that this platform can support supersonic flows lasting 35 ns in a counterpropagating geometry, and the

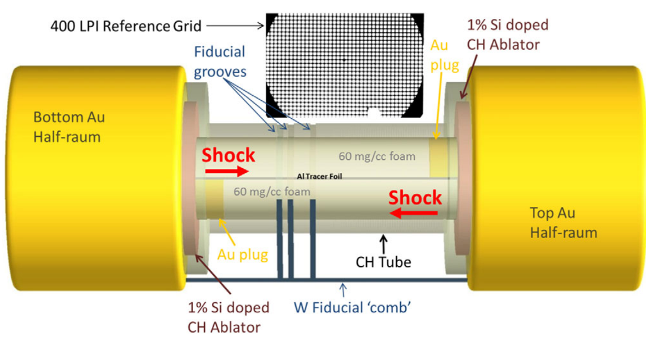

FIG. 1. Setup of the NIF shock-tube experiment showing the internal elements of the shock tube between the two 50 μm thick half-raum drivers, which are laser heated to 250 eV. The tube is made of 250 μm thick Be with an inner diameter of 1.5 mm and is 4.95 mm in length. The mixing tracer layer Al foil extends along the complete length of the tube past both Au plugs on opposite ends. The 170 μm thick ablators are doped with 2% silicon to reduce the M-band x-ray radiation from the half-raums which reduces the preheat of the experiments. The rest of the tube is filled with 60 mg/cc CH foam.

volume of this platform is large enough that edge effects and drive transients do not have time to propagate inward to interfere with the physics over the time scale over which the data are collected [8]. Varying the initial roughness on otherwise identical aluminum foils, we have observed a change in the behavior of the mixing layer as it is forced from typical Kelvin-Helmholtz (KH) coherent features [6,7], corresponding to an initial Reynolds number of $\sim 10^3$, to an increasingly turbulent behavior with highly stochastic features at an initial Reynolds number of $> 10^5$. Such a system has relevance to astronomical plasma shear flows, spanning the values thought to be present in protoplanetary accretion disks ($\mathrm{Re} \sim 10^3$) to protostellar accretion disks $\mathrm{Re} \gtrsim 10^{10}$ [9], and has implications for the persistence of initial conditions through instabilities in inertial confinement fusion research [10].

A body of recent and ongoing work, starting from George [2] in 1989, has shown the importance of initial conditions in fluid flows tending toward self-similarity, but not universal behavior. Slessor, Bond, and Dimotakis [11] showed that the profile of material mixing across a sheared mixing layer remains sensitive to the state of the fluid inflowing to the mixing layer, even under fully developed, self-similar conditions, and Pickett and Ghandhi [12] showed that "the mixed fluid profile was, therefore, not a unique function of local conditions, but remained sensitive to the state of the inlet conditions even in conditions considered to be fully developed." In particular, this sensitivity has been demonstrated to depend on whether or not the fluid flowing into the mixing layer's splitter-plate geometry was itself initially either laminar or turbulent. In addition, McMullan *et al.* [13] recently showed that initial conditions may even affect direct numerical simulations, the benchmark for turbulence calculations. What we present here shows that in our shock-driven HED mixing layer, which has a more than adequately developed dynamic Reynolds number ($\mathrm{Re}_d = 10^7$) to have evolved to be a fully turbulent mixing layer, the initial scale lengths set by the shock-surface interactions play the role of inflow condition scale lengths and influence the intermediate late time mixing of the developed flows.

Under HED conditions, i.e., > 1 eV and > 1 Mbar, Rayleigh-Taylor and Richtmyer-Meshkov hydrodynamic instabilities have been studied in several systems [14–16]. The KH shear instability has been less studied due to the more difficult geometry and time scales for supporting the flows. However, KH systems driven single sidedly by impulsive decaying shock waves have been studied previously and typically in only one of the two mixing materials or in the presence of imposed initial sinusoidal seed perturbations [17–23]. This platform [8,24,25] uses a 10 ns indirect drive from two sides to support the shocks during the experiment.

There are two important characteristics of the KH instability that deal with its interactions with the initial shearing interface: first, that there is no minimum unstable wave number, thus all seed wavelengths are in principle unstable; and second, that shorter-wavelength perturbations grow faster. This faster growth of smaller features is not typically seen in experiments because in a fluid, these features are often rounded, and are by nature not sharp interfaces. However, in an HED fluid experiment, the fluid starts off as a solid, which can be manufactured with extremely abrupt interfaces for initial conditions that vary both in the longitudinal and transverse directions in a broadband sense. However, in practice, this solid is initially flashed into a plasma (usually by laser-induced secondary radiation, e.g., hot electrons and/or soft x rays) on the order of an eV just as the experiment begins, which tends to erode the very small features as they heat and expand. Using this knowledge, we designed a set of experiments to take advantage of this characteristic by means of a roughened foil that would still leave relatively small sharp features to cause the instability to grow faster, and thus transition into a turbulent regime more quickly than the nominal smooth foil would. This is an analogous method to that of hypersonic turbulent boundary-layer tripping [26,27], where small features cause the flow to become turbulent.

Results.—Initial experiments were performed using the Omega Laser System driven directly by 5 kJ of laser energy on both sides. These experiments were reported in Doss *et al.* [28,29] and were well modeled using the RAGE [30] radiation hydrodynamics code running with the Besnard-Harlow-Rauenzahn (BHR) turbulent-mix model [31], an extended model of the $k - \epsilon$ type [32]. However, these experiments did not last long enough for a full determination of the late-time asymptotic behavior of the system. Thus, a similar experimental platform was developed for the NIF [8,24,25] using indirectly (soft x-ray) driven ablators. The platform is shown in Fig. 1, where we can image either the edge or plan view. The edge view uses x-ray radiography to look at the evolution of the foil mix width, and the plan view looks through the foil at the evolution of the structures on and in the foil, acquiring up to four images per shot at various times. Each half-raum produces a 250 eV thermal soft x-ray bath to drive 130 km/s shocks through the ablators into the system, producing 100 km/s flows on both sides of the shear tracer layer. This tracer layer is an Al foil with a nominal ~ 0.3 μm surface roughness (see Figs. 2 and 3).

Two roughnesses of Al foils were used, the nominal type with a smooth ~ 0.3 μm rms profile (Fig. 2) and the other type with an initially rough ~ 5 μm rms surface (Fig. 3). The smooth foil was cut from a simple rolled sheet of Al with an intrinsic surface roughness of no more than 0.4 μm rms. The roughened foil was created using a smooth foil with a coining technique, where the coining stamps were sand blasted with a grit of specific sizes to produce a roughened pattern of ~ 5 μm rms. The smooth Al foil was pressed between two patterned Al stamps to prevent contamination, and the resulting surface is shown in Figs. 3(a) and 3(b). These foils were initially tested using the Omega laser, and reported in Merritt *et al.*

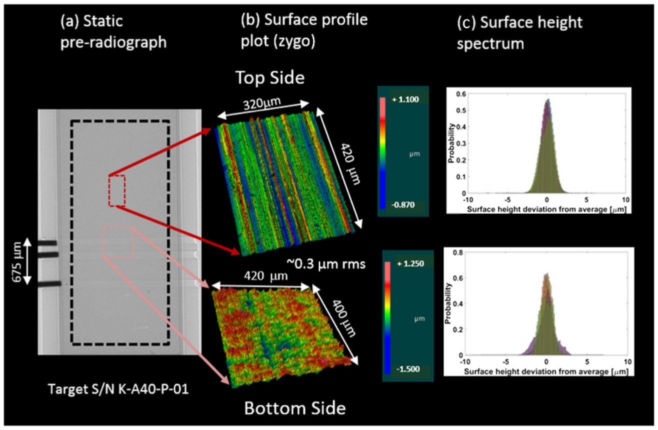

FIG. 2. Nominally smooth foil characteristics, showing an rms surface roughness of ∼0.3 μm.

[33], where the smooth foils did not exhibit the same coherent behavior as those reported here, because of the smaller experimental volume used there and additional transients.

The initial fluid Reynolds number can be used as a first guide to see how the system will evolve. We use the Braginskii plasma viscosity to calculate the initial Reynolds numbers. $\mathrm{Re}_0 = LU/\nu_0$, where L is the length scale, U is the flow velocity (ΔV for counterflowing geometries), and ν_0 is replaced by $\nu_0 = 0.96 n_{i0}\tau_0 kT = 1010(A^{1/2}T_0^{5/2})/(Z_0^4 \ln\Lambda)$ [cgs keV], where A is the ion species atomic number, T_0 is the initial ion temperature, Z_0 is the initial effective charge state, and $\ln\Lambda$ is the Coulomb logarithm (which is ∼1 for warm dense matter [34]). Both types of Al foils are heated to ∼50 eV when the shocks cross as determined by simulations. The flow velocity is 100 km/s on both sides of the foil after the shocks cross, which gives a ΔV of 200 km/s. The foil has an initial density of about 1 g/cc, and an initial effective Z_0 of 3. All scale lengths in the system are the same for both foils, other than the surface roughness, 5 and 0.3 μm rms (rough and smooth, respectively), which is also the initial seed of any instability on the interface of the foam and foil fluids, and thus is a natural choice to be used in calculating Re_0. For the smooth foil, one calculates an inflow $\mathrm{Re}_0 \sim 10^3$, which is high, but still in the classically not-fully-turbulent regime [35,36]. While for the rough foil, one calculates $\mathrm{Re}_0 \sim 10^5$, which is well into the classically turbulent flow regime. The overall mixing layer Reynolds number, calculated conventionally at late times using the overall dynamic mixing-layer width (∼300 μm) as the scale length [11,35], remains over 10^6, and is expected to be post-transition in both cases. Reference [8] has details about how the tracer mix layer evolves on the surface and in the bulk under KH shear, and can be thought of as a half-layer for the energy and mix analysis [25].

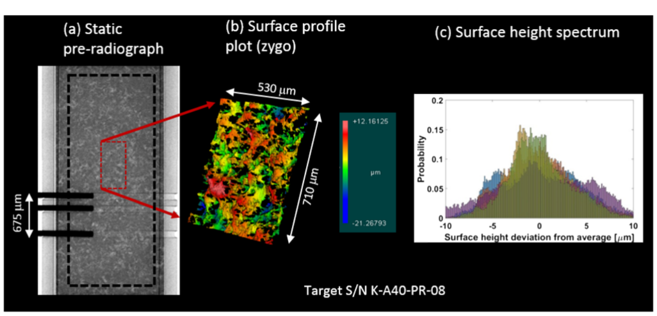

FIG. 3. Rough foil characteristics, showing an rms roughness of ∼5 μm.

A time history of the layer seen in Fig. 4 was compiled for both foils. The width of the mixing layer is measured using a 6.7 keV (Fe He-α) x-ray source, which produced 8 kJ of x rays [37], pinhole imaged onto a gated x-ray framing camera [38], taking 2 to 4 images per shot over 3–5 ns. The recorded images are shown in Fig. 5. An averaged lineout is taken at the center line of the experimental image from peak to 95% of peak and converted into a mix width. A similar procedure is followed for the simulation data output from the RAGE radiation hydrodynamics code [30]. From the experimental data and the simulations, curves of the simulated behaviors with and without a turbulent-mix model can be generated to compare to the data. Figure 4 shows simulations both with and without the BHR mix model [31] turned on at 18 ns, when mixing begins due to strong shear. When the mix model is turned on, the shear instability of the simulated layer can reproduce the behavior of the layers much better, particularly matching the asymptotic growth rate of the layer in both cases. In contrast, the lowest dashed line shows simulation without mix, which does not replicate any of the data.

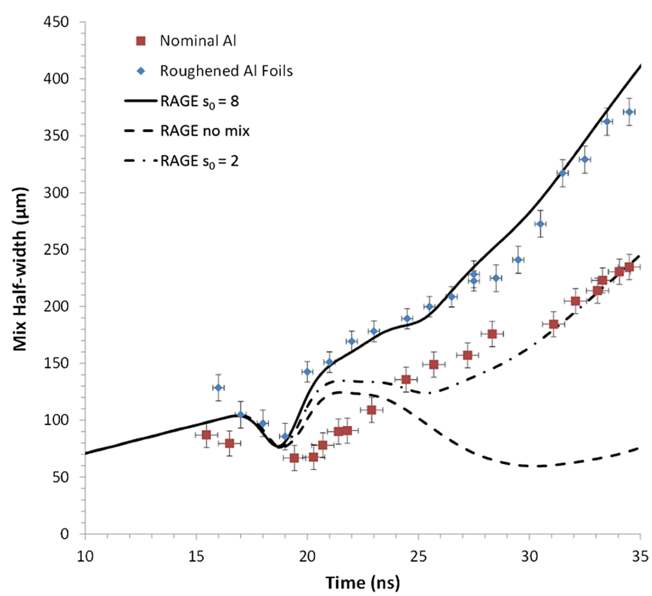

FIG. 4. Experimental data plotted with simulations results. Red squares are the nominally smooth Al data, blue diamonds are the roughened Al data. The solid black line is from the simulations with the BHR model using an $s_0 = 8$, the dot-dashed line is with the BHR model using an $s_0 = 2$, and the dashed line is the same simulation without the BHR model.

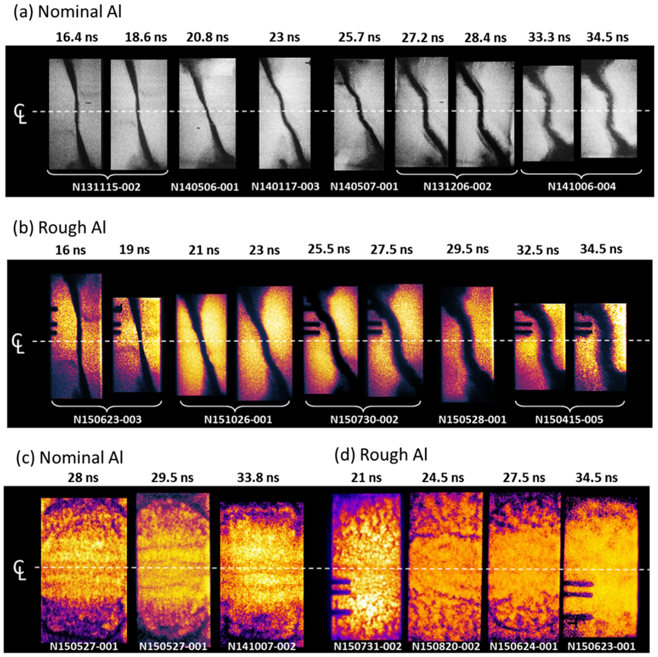

FIG. 5. (a) Edge views of nominally smooth Al, Ref. [8]; (b) edge views of rough Al; (c) plan views of nominally smooth Al; and (d) plan views of rough Al. Triplets of dark horizontal bars are tungsten alignment fiducials.

The BHR model is initialized with an initial scale length, denoted s_0, which sets the initial turbulent length scales and, at time zero, compares to the perturbations on the interfaces [39]. In the case of the nominal Al foil, this parameter needs to be set to 2 μm when the model is activated at 18 ns. For the roughened case, the parameter needs to be increased by a factor of 4. The asymptotic spreading rate of the layer is seen in both cases to become linear, as is expected of shear layers as they achieve self-similarity [11], yet at different rates.

We also call attention to the plan-view images in Figs. 5(c) and 5(d) of the two types of Al foils. We can see here that the smooth Al layer develops coherent structures, which are highly reminiscent of the traditional KH eddies, typically called rollers, seen in fluid hydrodynamic shear experiments [4–7]. These structures grow and can become quasisteady, and will strongly contribute to the growth of the mixing layer only after they saturate and energy begins to populate secondary instabilities which will merge the rollers and generate new eddies of smaller sizes [40–42] at later times. These secondary and tertiary mechanisms eventually populate the turbulent cascade, which will then finally speed up the mixing of materials across the layer [43]. Reference [8] shows in detail how we derive the dispersion relationship for the instabilities in this counterstreaming thin-tracer case.

When the tracer layer is changed from the smooth to the rough foil, the initial seeds are now much larger, yet small enough for strong growth, and are not washed out by the laser preheat which occurs in the layer. The small seeds of the rough foil (5 μm rms) stay relatively sharp, compared to the smaller seeds (0.4 μm rms) of the nominally smooth foil, and these larger seeds lead to broadband growth as expected in the system. This allows the system to keep adding energy into the mixing layer, causing it to expand at the code-predicted rate for a fully turbulent system. Looking at the plan views, Figs. 5(c)–5(d), there is an obvious difference between the smooth and the rough foil's behavior. In the smooth foil case, Fig. 5(c), there are dark bands near the center, which are persistent in time, indicative of KH eddies, i.e., rollers. In the rough foil case, Fig. 5(d), at an early time (21 ns) we can begin to see the growth of the same type of roller features seen in the smooth foil (at 28 ns), but the rough foil quickly becomes much more homogeneous with much more small scale cellularlike structures early in time (21–24.5 ns), washing out later in time (34.5 ns). Clearly, more energy is deposited into the layer as the rough layer grows much faster than the smoother layer as seen in Fig. 4. Strong (particularly spanwise) three-dimensional forcing is known in experiments to be capable of speeding the secondary instabilities and subsequent mixing [44,45]. In the smooth Al data, Fig. 5(c), one can see that the rollers are beginning to pair and kink at ~33.8 ns following the principal subharmonic instability [46] with a maximum growth rate of half that of the principal KH instability [40].

Conclusions.—In summary, we have shown that by changing the initial conditions of the foil roughness, from 0.4 to 5 μm rms, we are able to affect the evolution of the KH instability and the transition into a more mixed state of the tracer layer. In simulations, without the turbulent-mix model turned on, the layer does not expand, but is instead pressure balanced and does not grow significantly over 10 ns. Using the BHR mix model, the data are well matched for the case of the rough Al tracer layer, and are matched for late times for the smooth foil, when at those times more energy is transferred from the coherent structures to the turbulent field, where the initial conditions have less influence on the trajectory of the mix width as the system transitions to full turbulence. In inertial confinement fusion, the surface roughness of the fuel capsule is tightly controlled due to worries of instability growth and feedthrough to the central hot spot. If hydrodynamic mix is present and small features begin to grow instead of being washed out as is generally assumed, shear growth could lead to another significant source of mix into the fuel, especially when asymmetries arise, damping the energy and neutron yield. For the first time in an HED experiment, we have observed and demonstrated the transition of a system seeded with broadband structures from KH coherent structures to a system with a more homogeneous cellularlike structure indicative of strong mixing and turbulence, and matched the measured mix layer width to a simulation that has evolved from the same conditions using a turbulent-mix model.

The authors would like to thank the crew and support staff of the National Ignition Facility for operational and technical support. K. A. F. would like to thank Sandrine A. Gaillard for useful discussions and editing of the MS. This work was funded and carried out under the auspices of the U.S. Department of Energy by the Los Alamos National Laboratory under Contract No. DE-AC52-06NA25396, and by Lawrence Livermore National Laboratory under Contract No. DE-AC52-07NA27344.

*kflippo@lanl.gov
†fdoss@lanl.gov

[1] Y. B. Zeldovich, Zh. Eksp. Teor. Fiz. **7**, 1463 (1937) [*Selected Works of Yakov Borisovich Zeldovich*, edited by (Princeton University Press, Princeton, 1992), Vol. 1, pp. 82–85].
[2] W. K. George, in *Advances in Turbulence*, edited by W. K. George and R. E. A. Arndt (Hemisphere, New York, 1989), pp. 39–73.
[3] E. I. Moses and C. R. Wuest, Fusion Sci. Technol. **43**, 420 (2003).
[4] P. E. Dimotakis and G. L. Brown, J. Fluid Mech. **78**, 535 (1976).
[5] M. M. Rogers and R. D. Moser, J. Fluid Mech. **247**, 321 (1993).
[6] G. L. Brown and A. Roshko, J. Fluid Mech. **64**, 775 (1974).
[7] A. D'Ovidio and C. M. Coats, J. Fluid Mech. **737**, 466 (2013).
[8] F. W. Doss, J. L. Kline, K. A. Flippo, T. S. Perry, B. G. DeVolder, I. Tregillis, E. N. Loomis, E. C. Merritt, T. J. Murphy, L. Welser-Sherrill, and J. R. Fincke, Phys. Plasmas **22**, 056303 (2015).
[9] *Protostars and Planets VI*, edited by H. Beuther *et al.* (University of Arizona Press, Tucson, 2014).
[10] D. S. Clark, H. F. Robey, and V. A. Smalyuk, Phys. Plasmas **22**, 052705 (2015).
[11] M. D. Slessor, C. L. Bond, and P. E. Dimotakis, J. Fluid Mech. **376**, 115 (1998).
[12] L. M. Pickett and J. B. Ghandhi, Phys. Fluids **14**, 985 (2002).
[13] W. A. McMullan, S. Gao, and C. M. Coats, Int. J. Heat Fluid Flow **30**, 1054 (2009).
[14] A. J. Cole, J. D. Kilkenny, P. T. Rumsby, R. G. Evans, C. J. Hooker, and M. H. Key, Nature (London) **299**, 329 (1982).
[15] S. G. Glendinning, S. V. Weber, P. Bell, L. B. DaSilva, S. N. Dixit, M. A. Henesian, D. R. Kania, J. D. Kilkenny, H. T. Powell, R. J. Wallace, P. J. Wegner, J. P. Knauer, and C. P. Verdon, Phys. Rev. Lett. **69**, 1201 (1992).
[16] C. C. Kuranz, R. P. Drake, E. C. Harding, M. J. Grosskopf, H. F. Robey, B. A. Remington, M. J. Edwards, A. R. Miles, T. S. Perry, T. Plewa, N. C. Hearn, J. P. Knauer, D. Arnett, and D. R. Leibrandt, Astrophys. J. **696**, 749 (2009).
[17] E. C. Harding, J. F. Hansen, O. A. Hurricane, R. P. Drake, H. F. Robey, C. C. Kuranz, B. A. Remington, M. J. Bono, M. J. Grosskopf, and R. S. Gillespie, Phys. Rev. Lett. **103**, 045005 (2009).
[18] O. A. Hurricane, J. F. Hansen, H. F. Robey, B. A. Remington, M. J. Bono, E. C. Harding, R. P. Drake, and C. C. Kuranz, Phys. Plasmas **16**, 056305 (2009).
[19] O. A. Hurricane, V. A. Smalyuk, K. Raman, O. Schilling, J. F. Hansen, G. Langstaff, D. Martinez, H.-S. Park, B. A. Remington, H. F. Robey, J. A. Greenough, R. Wallace, C. A. Di Stefano, R. P. Drake, D. Marion, C. M. Krauland, and C. C. Kuranz, Phys. Rev. Lett. **109**, 155004 (2012).
[20] V. A. Smalyuk, O. A. Hurricane, J. F. Hansen, G. Langstaff, D. Martinez, H.-S. Park, K. Raman, B. A. Remington, H. F. Robey, O. Schilling, R. Wallace, Y. Elbaz, A. Shimony, D. Shvarts, C. Di Stefano, R. P. Drake, D. Marion, C. M. Krauland, and C. C. Kuranz, High Energy Density Phys. **9**, 47 (2013).
[21] L. Welser-Sherrill, J. Fincke, F. Doss, E. Loomis, K. Flippo, D. Offermann, P. Keiter, B. Haines, and F. Grinstein, High Energy Density Phys. **9**, 496 (2013).
[22] C. A. D. Stefano, G. Malamud, M. T. H. de Frahan, C. C. Kuranz, A. Shimony, S. R. Klein, R. P. Drake, E. Johnsen, D. Shvarts, V. A. Smalyuk, and D. Martinez, Phys. Plasmas **21**, 056306 (2014).
[23] W. C. Wan, G. Malamud, A. Shimony, C. A. D. Stefano, M. R. Trantham, S. R. Klein, D. Shvarts, C. C. Kuranz, and R. P. Drake, Phys. Rev. Lett. **115**, 145001 (2015).
[24] K. A. Flippo, F. W. Doss, B. Devolder, J. R. Fincke, E. N. Loomis, J. L. Kline, and L. Welser-Sherrill, J. Phys. Conf. Ser. **688**, 012018 (2016).
[25] F. W. Doss, K. A. Flippo, and E. C. Merritt, Phys. Rev. E **94**, 023101 (2016).
[26] S. A. Berry, A. D. Dilley, and J. F. Calleja, J. Spacecr. Rockets **38**, 853 (2001).
[27] Y. Zhao, W. Liu, D. Xu, D. Gang, and S. Yi, Acta Astronaut. **118**, 199 (2016).
[28] F. W. Doss, E. N. Loomis, L. Welser-Sherrill, J. R. Fincke, K. A. Flippo, and P. A. Keiter, Phys. Plasmas **20**, 012707 (2013).
[29] F. W. Doss, J. R. Fincke, E. N. Loomis, L. Welser-Sherrill, and K. A. Flippo, Phys. Plasmas **20**, 122704 (2013).
[30] M. Gittings, R. Weaver, M. Clover, T. Betlach, N. Byrne, R. Coker, E. Dendy, R. Hueckstaedt, K. New, W. R. Oakes, D. Ranta, and R. Stefan, Comput. Sci. Discovery **1** 015005 (2008).
[31] D. Besnard, F. Harlow, and R. Rauenzahn, Los Alamos National Laboratory Technical Report No. LA-10911-MS, 1987.
[32] B. E. Launder and D. B. Spalding, Comput. Methods Appl. Mech. Eng. **3**, 269 (1974).
[33] E. C. Merritt, F. W. Doss, E. N. Loomis, K. A. Flippo, and J. L. Kline, Phys. Plasmas **22**, 062306 (2015).
[34] J. D. Huba, *NRL Plasma Formulary* (Naval Research Laboratory, Washington, DC, 2011).
[35] P. E. Dimotakis, J. Fluid Mech. **409**, 69 (2000).
[36] Ye. K. Zhou, Phys. Plasmas **14**, 082701 (2007).
[37] K. A. Flippo, J. L. Kline, F. W. Doss, E. N. Loomis, M. Emerich, B. Devolder, T. J. Murphy, K. B. Fournier, D. H. Kalantar, S. P. Regan, M. A. Barrios, E. C. Merritt, T. S. Perry, I. Tregillis, L. Welser-Sherrill, and J. R. Fincke, Rev. Sci. Instrum. **85**, 093501 (2014).
[38] J. A. Oertel, R. Aragonez, T. Archuleta, C. Barnes, L. Casper, V. Fatherley, T. Heinrichs, R. King, D. Landers, F. Lopez, P. Sanchez, G. Sandoval, L. Schrank, P. Walsh, P. Bell, M. Brown, R. Costa, J. Holder, S. Montelongo, and N. Pederson, Rev. Sci. Instrum. **77**, 10E308 (2006).

[39] J. D. Schwarzkopf, D. Livescu, R. A. Gore, R. M. Rauenzahn, and J. R. Ristorcelli, J. Turbul. **12**, 1 (2011).
[40] R. T. Pierrehumbert and S. E. Widnall, J. Fluid Mech. **114**, 59 (1982).
[41] G. M. Corcos and S. J. Lin, J. Fluid Mech. **139**, 67 (1984).
[42] G. P. Klaassen and W. R. Peltier, J. Fluid Mech. **202**, 367 (1989).
[43] J. Jimenez, J. Fluid Mech. **132**, 319 (1983).
[44] R. W. Miksad, J. Fluid Mech. **56**, 695 (1972).
[45] J. C. Lasheras and H. Choi, J. Fluid Mech. **189**, 53 (1988).
[46] H. Lamb, *Hydrodynamics*, 6th ed. (Cambridge University Press, Cambridge, 1932).